

Gyrofluid Simulation of Ion-Scale Turbulence in Tokamak Plasmas[†]

Jiquan Li^{1,2,*} and Y. Kishimoto¹

¹ Graduate School of Energy Science, Kyoto University, Uji, Kyoto 611-0011, Japan.

² Institute for Fusion Theory and Simulation, Zhejiang University, Hangzhou, China.

Received 20 March 2008; Accepted (in revised version) 3 August 2008

Communicated by Zhihong Lin

Available online 9 September 2008

Abstract. An improved three-field gyrofluid model is proposed to numerically simulate ion-scale turbulence in tokamak plasmas, which includes the nonlinear evolution of perturbed electrostatic potential, parallel ion velocity and ion pressure with adiabatic electron response. It is benchmarked through advancing a gyrofluid toroidal global (GFT_G) code as well as the local version (GFT_L), with the emphasis of the collisionless damping of zonal flows. The nonlinear equations are solved by using Fourier decomposition in poloidal and toroidal directions and semi-implicit finite difference method along radial direction. The numerical implementation is briefly explained, especially on the periodic boundary condition in GFT_L version. As a numerical test and also practical application, the nonlinear excitation of geodesic acoustic mode (GAM), as well as its radial structure, is investigated in tokamak plasma turbulence.

PACS: 52.35.Kt, 52.35.Ra, 52.65.Tt, 52.55.Fa

Key words: Geodesic acoustic mode (GAM), zonal flow, ion temperature gradient (ITG) turbulence, gyrofluid simulation, tokamak.

1 Introduction

The study on turbulent particle and heat transport is of key importance for the improvement of confinement performance in magnetized fusion devices including current tokamaks/stellarators and the coming ITER. In a tokamak, plasma turbulence is rather copious in the spatio-temporal scale due to various linear and nonlinear instabilities. Typically the ion temperature gradient (ITG) driven turbulence is a representative of the ion-scale fluctuations. An important ingredient in turbulence is a poloidally and toroidally

[†]Dedicated to Professor Xiantu He on the occasion of his 70th birthday.

*Corresponding author. *Email addresses:* lijq@energy.kyoto-u.ac.jp (J. Li), kishimoto@energy.kyoto-u.ac.jp (Y. Kishimoto)

symmetric, coherent structure, namely the so-called zonal flow. A remarkable progress on understanding ion transport in tokamak plasmas has been achieved in past years through the extensive investigations on the ITG turbulence and the zonal flow dynamics. It is the very zonal flow that may regulate the ion-scale turbulence and reduce the ion transport to the neoclassical level observed in present tokamak experiments. Meanwhile, another large-scale structure, the so-called geodesic acoustic mode (GAM), has also attracted much attention recently. The GAM is a class of toroidal eigenmode with finite low frequency [1–4], which is characterized in spatial structure by poloidally and toroidally symmetric potential and poloidally asymmetric density or pressure fluctuations. The latter gives rise to a time-dependent zonal flow in toroidal plasmas. On the other hand, the GAM is a damped oscillator with finite frequency coupling with axisymmetrical static potential (i.e., the stationary zonal flows). The level of zonal flows in toroidal ITG turbulence is strongly influenced by the collisionless damping of the GAMs [5]. Hence, the GAM dynamics have been intensively studied in toroidal plasma experiments and large-scale parallel simulations in light of theoretical analyses [6–23].

To study the turbulent transport in tokamak plasma with the dynamics of zonal flows and GAMs, advanced numerical simulations based on modern gyrokinetic theory have been developed as the first principal simulation: particle-in-cell (PIC) and Continuum (Vlasov) approaches. These methods benefit from the dramatic progress of computational capacity although they are very CPU-time-consuming. On the other hand, the conventional computational fluid dynamics (CFD) is still a very useful method in plasma turbulence simulation to illustrate the complex nonlinear plasma interaction. An improved fluid version, which could properly involve the most important kinetic effects such as the finite Larmor radius (FLR) and Landau damping, has also been proposed and extensively testified. It is noticed that while this approximated approach has shown the advance in understanding the saturation mechanism and fluctuation characteristics of turbulence, the adequacy of the existent gyrofluid models for calculating the zonal flow damping is quite questionable and becomes a crucial failing. The zonal flow is inadequately damped due to the inappropriate closure of the moment hierarchy so that the transport is overestimated. This is still a remaining problem and the improved model is being chased [24–27]. In this paper, we propose a new gyrofluid closure relation for the zonal flow and GAM components. A toroidal global ITG code accompanying with a local version is advanced to benchmark the model with the theoretical prediction of the zonal flow damping. As a practical application, the nonlinear excitation of the GAM and its radial spectral characteristics are investigated.

The remainder of this paper is organized as follows: the new gyrofluid closure relation is proposed in Section 2 with the nonlinear governing equations of toroidal ITG turbulence. The numerical implementation for both global and local versions is briefly explained in Section 3, the benchmarking tests are presented. In Section 4, the nonlinear excitation is numerically simulated as a practical application of the newly developed gyrofluid modeling and codes. Finally, the summary is given in Section 5.

2 3-field gyrofluid ITG model in a tokamak plasma

The gyrofluid modeling has been well developed in plasma turbulence simulation [24–26]. However, a precise closure relation for lower order moment equations is still under improvement, especially for correct residual level of the zonal flows in ITG turbulence due to the collisionless GAM damping [27]. Here, we propose an empirical closure relation for the GAM components by considering the Landau damping and its parallel wavenumber, which may implicitly involve the effect of finite orbit width (FOW). Following the standard procedure [28], a set of three-field fluid equations of the normalized potential ϕ ; parallel ion velocity v_{\parallel} and ion pressure p_i can be derived as follows under the assumption of adiabatic electron response $n_e = (n_{eq}/T_{eq})(\phi - \langle \phi \rangle) = (n_{eq}/T_{eq})(1 - \delta)\phi$ [15, 16]

$$(1 - \delta - \nabla_{\perp}^2) \partial_t \phi = -(a/L_n) \nabla_{\theta} \phi - (1 + \eta_i)(a/L_n) \nabla_{\theta} \nabla_{\perp}^2 \phi - 2\Gamma \omega_D (\phi + p_i) - \frac{1}{2} \omega_D \nabla_{\perp}^2 \phi - \partial_r \langle \phi \rangle \nabla_{\theta} \phi - \nabla_{\parallel} v_{\parallel} + [\phi, \nabla_{\perp}^2 \phi] - \mu_{\perp} \nabla_{\perp}^4 \phi, \quad (2.1)$$

$$\partial_t v_{\parallel} = -\nabla_{\parallel} (\phi + p_i) - [\phi, v_{\parallel}] + \eta_{\perp} \nabla_{\perp}^2 v_{\parallel}, \quad (2.2)$$

$$\partial_t p_i = -(1 + \eta_i)(a/L_n) \nabla_{\theta} \phi - (\Gamma - 1/3) \Gamma (1 + \eta_i)(a/L_n) \nabla_{\theta} \nabla_{\perp}^2 \phi + 4\Gamma \omega_D p_i + (\Gamma - 1/2) \omega_D \nabla_{\perp}^2 \phi - \Gamma \nabla_{\parallel} v_{\parallel} - \gamma_{LD} \sqrt{8T_{eq}/\pi} |k_{\parallel}| (p_i - \phi) - [\phi, p_i] + \chi_{\perp} \nabla_{\perp}^2 p_i. \quad (2.3)$$

The normalized perturbed quantities are conventionally defined as [15]

$$(r; \nabla_{\perp}; \nabla_{\parallel}; t) \rightarrow (r/\rho_i; \rho_i \nabla_{\perp}; a \nabla_{\parallel}; t v_{ti}/a), \\ (n; \phi; v_{\parallel}; p_i) \rightarrow (a/\rho_i) (n/n_c; e\phi/T_{ic}; v_{\parallel}/v_{ti}; p_i/n_c T_{ic}).$$

Here the magnetic drift term is expressed as $\omega_D f = 2\varepsilon(\cos\theta \nabla_{\theta} + \sin\theta \nabla_r) f$ for any perturbed quantity f with $\varepsilon = a/R$. Heaviside step function $\delta = 0(1)$ is used for ITG fluctuations (the zonal flow component $\langle \phi \rangle$, $\langle \cdot \rangle$ denotes the flux surface average), which represents appropriately the adiabatic electron response to ITG fluctuations and the zonal flow. $\eta_i = L_{Ti}/L_n$ with $L_n = (d \ln n_{eq}/dr)^{-1}$ and $L_{Ti} = (d \ln T_{eq}/dr)^{-1}$, i.e., the characteristic length of equilibrium density (and ion temperature); $\rho_i = v_{ti}/\omega_{ci}$ ion Larmor radius with ion cyclotron frequency $\omega_{ci} = eB_0/m_i$. μ_{\perp} , η_{\perp} and χ_{\perp} are the numerical normalized cross-field viscosities and thermal conductivity, which can absorb the energy cascaded to short wavelength region. The dominant nonlinear terms come from the $\vec{E} \times \vec{B}$ convective nonlinearity, which are expressed by the Poisson bracket $[f, g] = (\partial_r f \partial_{\theta} g - \partial_{\theta} f \partial_r g)/r$ in circular tokamak geometry (r, θ, ζ) with the radius of the magnetic surface r , the poloidal and toroidal angles θ and ζ , respectively. In this work, $\Gamma = 5/3$ and $\tau = 1$ are used.

The kinetic Landau damping physics is also represented by Hammett-Perkins closure model for the parallel heat flux moment $q_{\parallel} = -i\gamma_{LD} \sqrt{8T_{eq}/\pi} k_{\parallel} T_i / |k_{\parallel}|$ [24]. However, the coefficients γ_{LD} for the ITG fluctuations and for the GAM components are different. It is

empirically determined as

$$\gamma_{LD} = \begin{cases} \Gamma - 1 & \text{for ITG,} \\ 3\Gamma & \text{for GAMs.} \end{cases} \quad (2.4)$$

Further, the parallel wavenumber for the GAMs is chosen with the parametric dependence of the safety factor q and the inverse aspect ratio ε , which may *implicitly* involve the FOW effects.

$$\nabla_{\parallel} = ik_{\parallel} = \begin{cases} \varepsilon(\partial_{\theta}/q + \partial_{\zeta}) & \text{for ITG,} \\ (3+\Gamma)(q/1.6)^{1/4} \varepsilon^{1/2} (\varepsilon \partial_{\theta}/q) & \text{for GAMs.} \end{cases} \quad (2.5)$$

It is noticed that the coefficients in Eqs. (2.4) and (2.5) for the GAMs are still adjustable, which depend on the nonlinear modification of pressure profile.

3 Numerical implementation and benchmarking test

3.1 Numerical algorithm

The nonlinear equations (2.1)-(2.3) in a tokamak plasma can be numerically solved using a conventional hybrid finite-difference spectral method in a toroidal geometry (r, θ, ζ) . Usually the Fourier decomposition in poloidal and toroidal directions are applied for any perturbed variable $f(t, r, \theta, \zeta)$, i.e.,

$$f(t, r, \theta, \zeta) = \sum_{m,n} f_{m,n}(t, r) \exp[i(m\theta - n\zeta)]. \quad (3.1)$$

Here the poloidal and toroidal mode numbers (m, n) are any integer but satisfy positive safety factor $q = m/n$ for the resonant modes with $\nabla_{\parallel} f = 0$. The components with $n = 0$ correspond to the non-resonant modes. For example in this paper, the potential $\phi_{0,0}$ is the zonal flow and the pressure $p_{0,0}$ is identical to the nonlinear modification of radial profile. The pressure components $p_{\pm 1,0}$ coupling with $\phi_{0,0}$ represent the so-called GAM. (Precisely speaking, the GAM perturbation also includes all toroidally symmetrical components $p_{\pm m,0}$ due to the geometrical coupling). For large-scale simulation with high resolution, the nonlinear terms are computed in real space using a de-aliased fast Fourier transform (FFT) algorithm and then transforming back to Fourier space with an inverse FFT while the linear terms are calculated in Fourier space. This is more efficient way for the calculation of quadratic nonlinearity in plasma turbulence. In the radial direction, centred finite-differences are employed to calculate the derivatives. Hence the resulting code is the second order accurate in space. The differential operators in space are expressed as

$$\nabla_{\perp}^2 f = \partial_r (r \partial_r) / r - m^2 / r^2, \quad (3.2)$$

$$\nabla_{\parallel} = ik_{\parallel} = \begin{cases} (i\varepsilon/q)(m - nq) & \text{for ITG,} \\ (3+\Gamma)(q/1.6)^{1/4} \varepsilon^{1/2} (i\varepsilon m/q) & \text{for GAMs.} \end{cases} \quad (3.3)$$

The magnetic drift term is expressed as the toroidal coupling of poloidal components

$$\omega_D f_{m,n} = i\varepsilon [m(f_{m+1,n} + f_{m-1,n}) - (\partial_r f_{m+1,n} - \partial_r f_{m-1,n})]. \quad (3.4)$$

The scheme for time integration is more considerable due to the different physical time scales in the model equation system. In a tokamak plasma with strong equilibrium magnetic field, the perpendicular frequency of the ion-scale fluctuation is estimated essentially by ion diamagnetic frequency while the parallel time scale is determined by the sound waves. The short parallel wave-length components with fast time scale are not much interesting in ion-scale turbulence of tokamak plasma and they are also dissipated rapidly by the Landau damping although the gyrofluid model is still rough. For the interested wavelengths, the parallel time scale is longer or comparable to the perpendicular one. We choose the time step determined by the latter with a sufficient accuracy. On the other hand, a hyper-viscosity dissipation is still kept in the gyrofluid model for numerical consideration although the FLR effect has been improved in the model. This may introduce a numerical instability on the transport scale for larger viscosity. Hence we adopt an explicit second (or/and fourth) order Runge-Kutta or Lax-Wendroff scheme for the perpendicular and parallel dynamics. An implicit scheme with a Crank-Nicolson method is adopted to avoid the possible numerical instability. Namely, a semi-implicit scheme is employed.

Here it is worthwhile to explain the treatment of the boundary condition. In the global code (GFT_G) for plasma microturbulence, the resonant modes are generally arranged in a toroidal annulus of $r_b \leq r \leq r_a$ considering linearly more unstable region. Here we set $0 < r_b \leq 0.2$ and $0.8 \leq r_a < 1$. Obviously, the periodic boundary condition for all variables is naturally satisfied due to the Fourier expansion along the poloidal and toroidal directions. In the radial direction, all fluctuating quantities are set to zero at the boundaries. The (0,0) components of the potential, parallel velocity and ion pressure are assumed to zero at outer boundary $r=r_b$ and their radial derivatives are set to zero at the inner $r=r_a$. In some case, a fixed pressure profile is taken by artificially removing the component $p_{(0,0)}$ to avoid the quasilinear flattening (QLF) effect or model the external heating.

On the other hand, in the local version (GFT_L) of the code, plasma profile effect is removed except for the gradient. The fixed boundary conditions are not applicable for all fluctuating components and also for the (0,0) modes due to the probably non-physical QLF effect. The periodicity boundary condition is one option to calm the QLF effect. The heat flowing out of one side re-enters into another side so that the temperature remains the average gradient everywhere in the simulation domain. However, the periodicity boundary condition is not simply implemented by directly connecting the corresponding variables at two boundaries in a sheared magnetic geometry. The difficulty in 3-dimensional tokamak plasma simulation comes from the magnetic shear. The fluctuations tend to be elongated along the magnetic field line, which points in different direction at different radii after one period along the toroidal direction. The magnetic field is twisted with a shear and the fluctuation at the end of a toroidal period seems

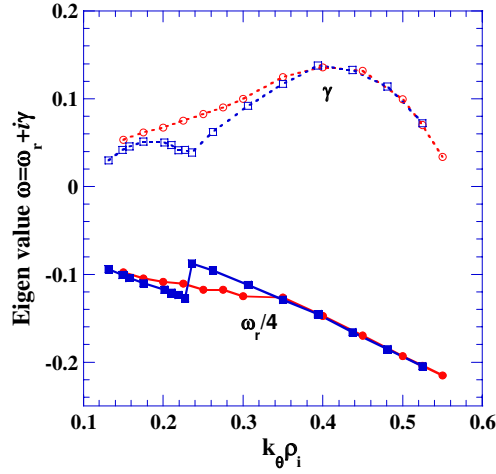


Figure 1: Growth rate and real frequency of toroidal ITG modes under the standard Cyclone base case parameters: $L_{Ti}/R = 6.9$, $L_n/R = 2.2$, $a/R = 0.18$, $q = 1.4$, $\hat{s} = 0.78$. Numerical parameters are chosen as $\mu_{\perp} = \eta_{\perp} = \chi_{\perp} = 0.8$. The square-marked curves correspond to the global results from GFT_G, the circle-marked ones are the corresponding local results from GFT_L.

to be radially shifted to connect another one. Corresponding to the ballooning representation, the radial periodicity in real space means a shift of poloidal number for each toroidal mode. The shift is determined by the magnetic shear. For the convenience, we move the toroidal geometry to a curved 3D slab at around a reference surface $r = r_0 = a/2$. The radial domain becomes $L_x = (r_b - r_a)a$ and the toroidal mode number in the toroidal coordinate corresponds to the wave-number m_y in y direction of curved slab geometry due to $q_0 = m_0/n_0$. Hence the wave-number m_z in z direction determines the resonant surface of each poloidal harmonic locally. The radial periodicity boundary condition can be expressed as

$$f_{m_y+m_s, m_z}(x+L_x) = f_{m_y, m_z}(x), \quad (3.5)$$

with $m_s = m_y \hat{s} L_x L_z / L_y$ being an integer. Here the magnetic shear $\hat{s} = r q' / q$, L_y and L_z are the domain size in y and z directions, respectively. This is similar to the treatment in the quasiballooning coordinate [29]. It is also equivalent to the method in a flux tube simulation [25].

3.2 Benchmarking test

The standard Cyclone base case parameters have been extensively applied to benchmark newly developed kinetic codes [30]. However, it is difficult to precisely benchmark a three-field fluid and/or gyrofluid model due to the low-order moment closure relation for finite Larmor radius (FLR) effects. In Eqs. (2.1)-(2.3), several additional terms, which represent more precise FLR effects, have been incorporated to have a correct spectral structure of linear ITG instability. We have applied the Cyclone base case parameters to both GFT_G and GFT_L versions to calculate linear ITG instability. Fig. 1 displays the

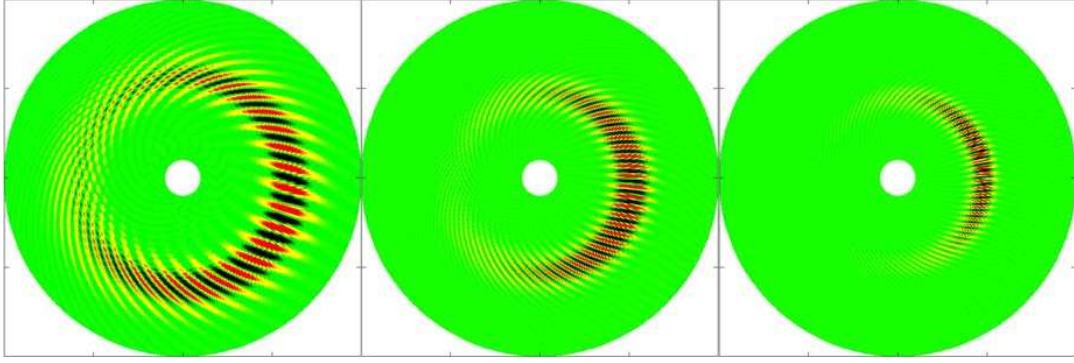


Figure 2: Eigenfunctions of toroidal ITG mode for different toroidal mode number $n=20$ (left); $n=40$ (center) and $n=60$ (right). The corresponding wavenumbers are $k_{\theta\rho_i}=0.175$; 0.35 and 0.525. The standard Cyclone base case parameters are used: $L_{Ti}/R=6.9$, $L_n/R=2.2$, $a/R=0.18$, $q=1.4$, $\hat{s}=0.78$. $\mu_{\perp}=\eta_{\perp}=\chi_{\perp}=0.8$, $a/\rho_i=320$.

eigen frequency and growth rate of toroidal ITG mode under the standard Cyclone base case parameters: $L_{Ti}/R=6.9$, $L_n/R=2.2$, $a/R=0.18$, $q=1.4$, $\hat{s}=rq'/q=0.78$. Here the characteristic lengths of density and temperature and the magnetic shear are taken at local region with maximum pressure gradient. The profiles of the safety factor q , the density and ion temperature are assumed as [31]

$$\begin{aligned} q(r) &= 0.854 = 2.184(r/a)^2, \\ n(r) &= n_0 \exp\{-0.667\epsilon \tanh[(r/a-0.5)/0.3]\}, \\ T_i(r) &= T_{i0} \exp\{-2.076\epsilon \tanh[(r/a-0.5)/0.3]\}. \end{aligned}$$

Note that the maximum growth rate and corresponding frequency are close to the kinetic values near the spectral peak $k_{\theta\rho_i} \approx 0.4$. The global mode structure near the surface of maximum pressure gradient exhibits strong ballooning characteristics, as shown in Fig. 2, which is comparable to the results based on a gyrokinetic Vlasov simulation [31]. It is also noticed that in the global calculations, a discontinuity of the eigenvalues versus $k_{\theta\rho_i}$ appears around $k_{\theta\rho_i} \approx 0.23$. This phenomenon may come from a local singularity of the fluid model (likely fluid resonance) due to the global profile for some cases of parameter. Since the fluid/gyrofluid model truncates the moment chain so that a fluid resonance may be unexpectedly brought in lower order fluid model such as this 3-field equation system, which also depends on the parameters. In a global simulation, it probably occurs due to the involvement of radial profile. It has been observed that a broken ballooning structure locally appears for the parameters around $k_{\theta\rho_i} \approx 0.23$. In this case, the lower order fluid/gyrofluid equation system should be improved to include some higher order fluid moments, such as the 4-field or 6-field gyrofluid model [25]. This issue will be discussed in future publications.

The most important motivation for developing these gyrofluid codes is to correctly calculate the zonal flow level in tokamak ITG turbulence. The residual zonal flow in tur-

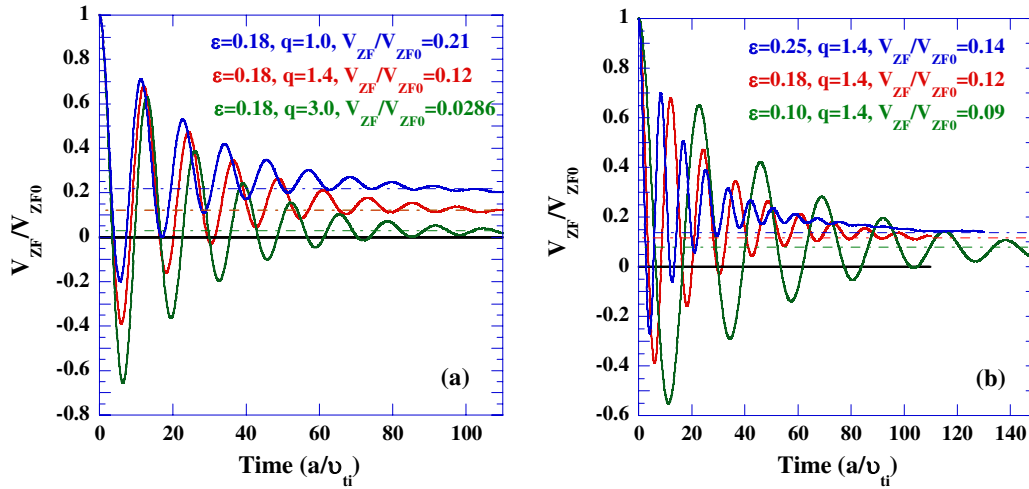


Figure 3: Time evolution of an initial static zonal flow $V_{ZF0}(t=0) = \sin(0.19x)$ in the zonal flow damping tests for different q values with $\epsilon=0.18$ (a) and for different ϵ values with $q=1.4$ (b).

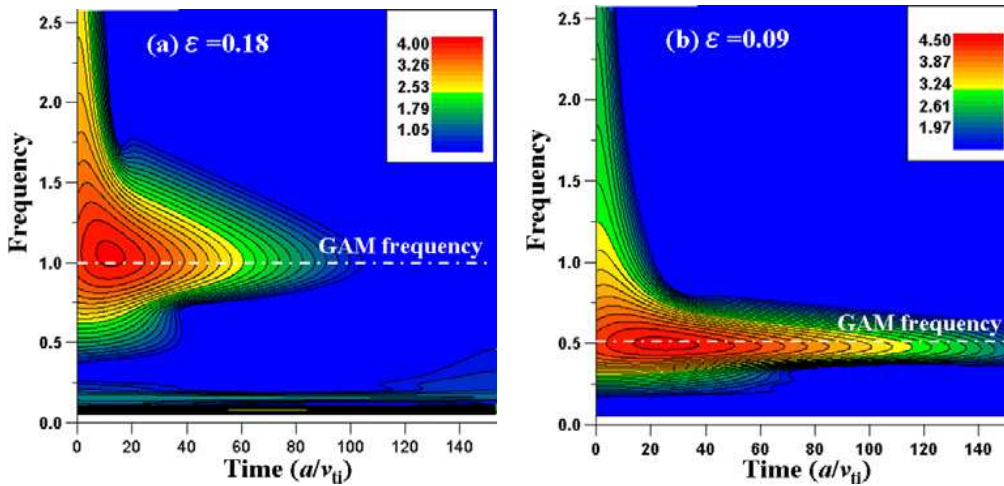


Figure 4: Wavelet energy analysis for the zonal flow damping. It produces clearly the parametric dependence of the GAM frequency on the inverse aspect ratio, i.e., $\omega_{GAM} \propto \epsilon(=a/R)$. $\epsilon=0.18$ (a) and $\epsilon=0.09$ (b). The initial static zonal flow is assumed as $V_{ZF0}(t=0) = \sin(0.19x)$, $q=1.4$. The contours indicate the spatially averaged $\ln(\langle \phi_{ZF}^2/2 \rangle)$ in the frequency-time plane.

bulent fluctuations determines the regulation of turbulence and the anomalous transport. It sensitively depends on the collisionless Landau damping due to the toroidal coupling with the GAMs. To have a suitable coefficient of the closure relation for the GAMs, an initial value test for the zonal flow damping is performed by comparing the residual zonal flows with the analytical theory under the Cyclone base case parameters. Fig. 3 illustrates the residual level of the zonal flows for different parameters q and ϵ . It can be seen

that the new closure relation shows the zonal flow damping and a correct residual level, which are well in agreement with the theoretical prediction $V_{ZF} = (1 + 1.6q^2/\varepsilon^{1/2})^{-1}V_{ZF0}$ by Rosenbluth and Hinton [32]. The wavelet energy analysis as shown in Fig. 4 also clearly exhibits the zonal flow damping process and the parametric dependence of the GAM frequency on $\varepsilon = a/R$.

4 Nonlinear excitation of GAMs in ITG turbulence

The GAM is a damped eigenmode in toroidal plasmas, which is coupled with axisymmetrical static potential through the geodesic curvature. The generation mechanism and/or the excitation process of the GAMs become an interesting topic in theory and experiments. Generally, the GAM oscillation can be kicked through a static potential like an initial stationary zonal flow or a stationary pressure ripple. It is quickly damped through the Landau damping and the coupling with ion sound wave (SW). The decay rate is roughly estimated as $\propto q^5 \exp(-\alpha q^2)$ with constant α for small drift orbits [20, 23]. It is believed that the GAMs can be excited nonlinearly through the Reynolds stress like the stationary zonal flows. Based on Eqs. (2.1)-(2.3), the GAM oscillator and the nonlinear source terms are expressed as follows

$$-\nabla_{\perp}^2 \partial_t \phi_{(0,0)} = -2\Gamma\omega_D(\phi + p_i)_{(\pm 1,0)} - \frac{1}{2}\omega_D \nabla_{\perp}^2 \phi_{(\pm 1,0)} + [\phi, \nabla_{\perp}^2 \phi]_{(0,0)}, \quad (4.1)$$

$$\begin{aligned} \partial_t p_{i(\pm 1,0)} = & 4\Gamma\omega_D p_{i(0,0)} + \left(\Gamma - \frac{1}{2}\right)\omega_D \nabla_{\perp}^2 \phi_{(0,0)} - \Gamma \nabla_{\parallel} v_{\parallel(\pm 1,0)} \\ & - \gamma_{LD} \sqrt{\frac{8}{\pi}} |k_{\parallel}| (p_i - \phi)_{(\pm 1,0)} - [\phi, p_i]_{(\pm 1,0)}. \end{aligned} \quad (4.2)$$

In addition, the equations of $\phi_{(\pm 1,0)}$ and $v_{\parallel(\pm 1,0)}$ should be also incorporated to have a coupled system of the GAMs, ion SWs and the zonal flows. When the nonlinear terms are ignored, the damped GAM oscillator accompanied by the ion SW is established with the frequency ω_{GAM} . Here we will simulate the nonlinear excitation of the GAMs due to the ITG fluctuations.

The GAMs are the combination of the perturbation of $(m,n)=(0,0)$ and $k_r \neq 0$ in potential field and the perturbation of $(m,n)=(\pm 1,0)$ and $k_r \neq 0$ in the density and/or pressure fields. The former is mixed by the stationary zonal flows and the components with finite low frequency ω_{GAM} . The radial structure of the GAMs may also be different from the counterpart of the zonal flows. Hence, the zonal flow component $\phi_{(0,0)}$ is composed in a general sense by two parts with different frequencies, i.e.,

$$\phi_{(0,0)} = \lambda_{ZF}\phi_{(0,0)}(\omega=0) + \lambda_{GAM}\phi_{(0,0)}(\omega=\omega_{GAM}). \quad (4.3)$$

The ratio of the two parts is determined by the balance between the driving force and damping sink of the GAMs. The stationary part of the zonal flows is commonly generated nonlinearly through a modulational instability [4]. Meanwhile, it also suffers from the collisionless damping due to the coupling with the GAMs. For the part with GAM

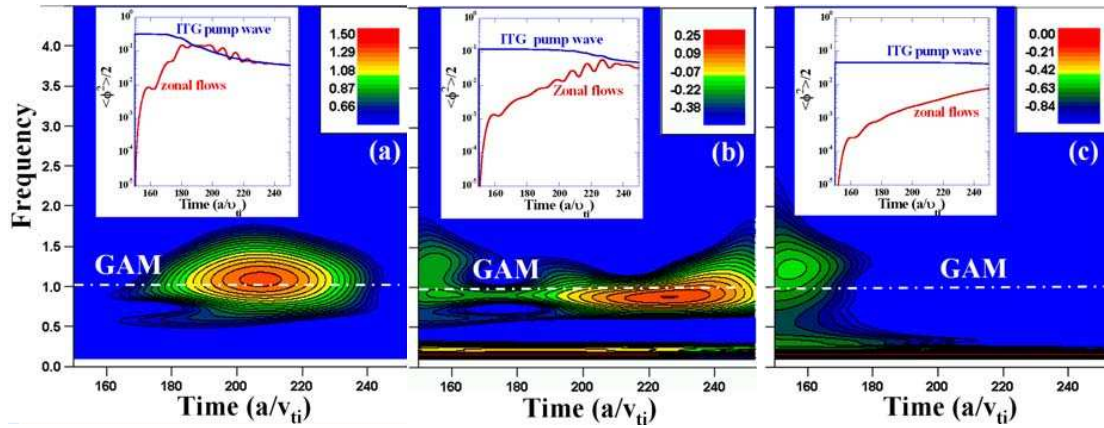


Figure 5: Wavelet energy analyses for the nonlinear excitation of the GAMs in high q plasmas ($q=2.6$) by the ITG fluctuation with different pump amplitude level $\langle \phi_{ITG}^2/2 \rangle \approx 0.3$ (a); 0.12 (b); 0.047 (c). The contours exhibit the spatially averaged $\ln(\langle \phi_{ZF}^2/2 \rangle)$ in the frequency-time plane. Note that the nonlinear excitation of GAM instability depends on the ITG pump amplitude. The inset graphs are the corresponding time evolution of total zonal flow energy and the pump wave. The standard Cyclone base case parameters are used here except for q value.

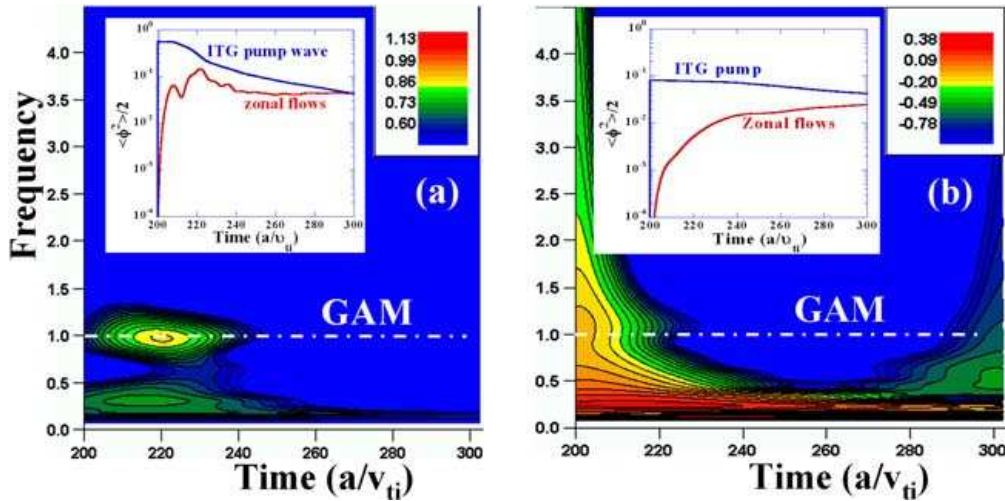


Figure 6: Wavelet energy analyses for the nonlinear excitation of the GAMs in low q plasmas ($q=1.0$) by the ITG fluctuation with different pump amplitude level $\langle \phi_{ITG}^2/2 \rangle \approx 0.58$ (a); 0.082 (b). The standard Cyclone base case parameters are used here except for q value.

frequency, it may be driven nonlinearly through a parametric instability [25], namely 3-wave interaction, due to the finite frequency. The parametric instability may involve the nonlinear terms $[\phi, p_i]_{(\pm 1, 0)}$, $[\phi, v_{||}]_{(\pm 1, 0)}$ and $[\phi, \nabla_{\perp}^2 \phi]_{(\pm 1, 0)}$ as well as the coupling with the Reynolds stress $[\phi, \nabla_{\perp}^2 \phi]_{(0, 0)}$. The parametric instability results from the balance between the nonlinear driving and the Landau damping as well as the coupling with the ion SW.

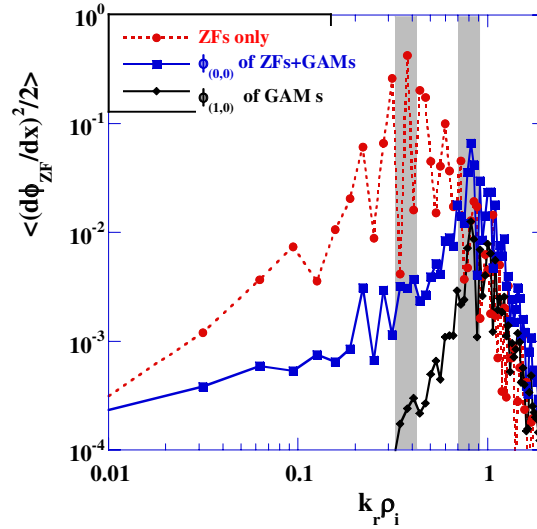


Figure 7: Radial spectra of the zonal flows in the simulations without (closed circles) and with (closed squares) the GAMs. The curve with diamonds corresponds to that of $d\phi_{(\pm 1,0)}/dx$ component of the GAMs. The standard Cyclone base case parameters are used in both simulations except for $q=2.0$ and $k_\theta \rho_i=0.35$.

To have a direct simulation of the nonlinear excitation of the GAMs in ITG turbulence, several simulations have been designed to investigate the detailed physics processes.

The GAMs are robust in toroidal plasmas with higher q [15, 16]. To observe the parametric instability of the GAMs, ITG fluctuations with different amplitude are provided as the pump wave. In these simulations, linear ITG modes are initially excited to some level and then artificially controlled to keep a constant amplitude. In such a quasi-steady ITG fluctuation, the nonlinear excitation of the zonal flows with the GAMs can be analyzed by choosing different ways for the comparison. Fig. 5 shows the dependence of the nonlinear excitation of the GAMs on the ITG pump amplitude. The inset graphs illustrate the time evolution of total zonal flow energy and the pump waves. It can be seen that the GAM instability becomes weaker as the ITG pump amplitude decreases. Further, the GAM fluctuation may be stabilized or damped even if the zonal flows still grow up for lower ITG pump amplitudes, indicating that the pump amplitude threshold for the GAM instability is higher than that of the zonal flow instability. This is understandable at least since the GAMs suffer from strong Landau damping. As the ITG pump amplitude becomes lower, weak GAMs are initially produced only through the beat wave of the pump fluctuations and strongly damped as shown in Fig. 5(c). In addition, the zonal flow energy decreases after the saturation due to the collisionless damping of the GAMs. Hence, the GAMs are difficult to survive in turbulent fluctuations if there exists no enough strong nonlinear driving force.

On the other hand, for the plasmas with lower q values, weak GAM instability can be observed only in higher ITG pump amplitude case, and it is quickly damped after the zonal flow saturation, as shown in Fig. 6(a). For the ITG pump wave with low ampli-

tude, the GAM fluctuation is almost damped. A reference simulation without the GAM components is performed for the comparison with Fig. 6(b). It shows that the damped GAMs can efficiently reduce the zonal flow instability and the suppression role in ITG fluctuations even if they are very weak.

The GAM fluctuations are characterized by finite low frequency in the zonal flow potential and the perturbed components with $(m, n) = (\pm 1, 0)$. They also possess a radial structure. Two local simulations are performed for the cases without and with the GAMs under the Cyclone base case parameters for the most unstable ITG mode $k_\theta \rho_i = 0.35$ to compare the difference of the zonal flows and the GAMs. It is observed that the radial structure of the GAMs is shorter than that of the pure zonal flow fluctuation as shown in Fig. 7. This result approaches the observation $k_r \rho_i \sim 1.0$ in the global ITG simulation [16]. Note that some scaling of the radial structure of the GAMs has been also estimated as $k_r \rho_i \propto L_T^{1/3}$ or $L_n^{1/3}$ [21, 33]. Some simulations with different L_T/R have been done and the results show almost the same spectra of the GAMs.

5 Summary

The precise gyrofluid model is helpful in large-scale turbulence simulations and physics analyses. In this work, a new empirical closure relation for the conventional three-field gyrofluid model is presented with emphasizing the zonal flow residual level due to the collisionless damping. A gyrofluid toroidal global ITG code (GFT_G) and the local version (GFT_L) have been developed. It is shown that the model can well reproduce the linear spectra of the toroidal ITG mode and the ballooning structures under the standard Cyclone base case parameters. The simulation tests for the zonal flow damping show that the key parametric dependence of the residual level of the static zonal flows on both the safety factor and the inverse aspect ratio is in agreement with the analytical prediction of the gyrokinetic theory.

As an application of the newly developed gyrofluid modeling, the nonlinear excitation of the GAMs is simulated in toroidal ITG turbulence. The spatio-temporal spectra of the zonal flows with the GAM components are analyzed by using time-dependent wavelet energy analysis. It is examined that the damped GAMs can be nonlinearly driven to excite an instability by an ITG pump wave with larger amplitude, which is higher than the pump amplitude threshold of the zonal flow instability. Furthermore, it is found that the radial structure of the GAMs is scaled as $k_r \rho_i \leq 1.0$, which is shorter than that of the pure zonal flows.

Acknowledgments

J. L. would like to thank Liu Chen for the suggestion and discussion. This work was supported by the Grant-in-Aid from Japan Society for the Promotion of Science (No. 18340186

and 19560828), and partly by the National Science Foundation of China Grant No. 10575032 and by the JSPS-CAS Core University Program (CUP) on Plasma and Nuclear Fusion.

References

- [1] Winsor N, Johnson J L and Dawson J M, 1969 Phys. Fluids 11 2448.
- [2] Hallatschek K and Biskamp D 2001 Phys. Rev. Lett 86 1223.
- [3] Itoh K, Hallatschek K and Itoh S-I, 2005 Plasma Phys. Controlled Fusion 7 635.
- [4] Diamond P H, Itoh S-I, Itoh K and Hahm T S, 2005 Plasma Phys. Controlled Fusion 47 R35.
- [5] Miki K, Kishimoto Y, Miyato N and Li J Q 2007 Phys. Rev. Letts. 99 145003.
- [6] Shats M G and Solomon W M 2002 Phys. Rev. Letts. 88 045001.
- [7] McKee G R et al. 2003 Phys. Plasmas 10 1712.
- [8] Fujisawa A et al. 2004 Phys. Rev. Lett. 93 165002.
- [9] Conway G D et al. 2005 Plasma Phys. Control. Fusion 47 1165.
- [10] Zhao K J et al. 2006 Phys. Rev. Lett. 96 255004.
- [11] Kramer-Flecken A. et al. 2006 Phys. Rev. Lett. 97 045006.
- [12] Ido T et al. 2006 Nucl. Fusion 46 512.
- [13] Hamada Y et al. 2007 Phys. Rev. Letts. 99 065005.
- [14] Scott B. 2003 Phys. Lett. A 320 53.
- [15] Miyato N, Kishimoto Y and Li J Q 2004 Phys. Plasmas 11 5557.
- [16] Miyato N, Kishimoto Y and Li J Q 2006 Plasma Phys. Controlled Fusion 48 A335.
- [17] Naulin V. et al 2005 Phys. Plasmas 12 052515.
- [18] Kendl A and Scott B D 2005 Phys. Plasmas 12 064506.
- [19] Watari T, Hamada Y, Notake T, Takeuchi N and Itoh K 2006 Phys. Plasmas 13 062504.
- [20] Gao Z, Itoh K, Sanuki H and Dong J Q 2005 Phys. Plasmas 12 064506.
- [21] Chakrabarti N, Singh R, Kaw P K and Guzdar P N, 2007 Phys. Plasmas 14 052308.
- [22] Berk H L et al. 2006 Nucl. Fusion 46 S888.
- [23] Chen L and Zonca F, Radial structures and nonlinear excitation of Geodesic Acoustic Modes, Sherwood 2007.
- [24] Hammett G W and Perkins F W 1990 Phys. Rev. Lett. 64 3019.
- [25] Beer M A and Hammett G W 1996 Phys. Plasmas 3 4046.
- [26] Sugama H, Watanabe T H and Horton W 2001 Phys. Plasmas 8 2618.
- [27] Sugama H, Watanabe T H and Horton W 2007 Phys. Plasmas 14 022502.
- [28] Horton W 1990 Phys Reports 192 1.
- [29] Dimits A M 1993 Phys. Rev. E 48 4070.
- [30] Dimits A M, Bateman G, Beer M A et al. 2000 Phys. Plasmas 7 969.
- [31] Idomura Y, Tokuda S and Kishimoto Y 2003 Nucl. Fusion 43 234.
- [32] Rosenbluth M N and Hinton F L 1998 Phys. Rev. Lett. 80 724.
- [33] Itoh S-I, Itoh K, Sasaki M, Fujisawa A, Ido T and Nagashima Y 2007 Plasma Phys. Controlled Fusion 49 L7.